

Slip Suppression Sliding Mode Control with Various Chattering Functions

Shun Horikoshi, Tohru Kawabe

Abstract—This study presents performance analysis results of SMC (Sliding mode control) with changing the chattering functions applied to slip suppression problem of electric vehicles (EVs). In SMC, chattering phenomenon always occurs through high frequency switching of the control inputs. It is undesirable phenomenon and degrade the control performance, since it causes the oscillations of the control inputs. Several studies have been conducted on this problem by introducing some general saturation function. However, study about whether saturation function was really best and the performance analysis when using the other functions, weren't being done so much. Therefore, in this paper, several candidate functions for SMC are selected and control performance of candidate functions is analyzed. In the analysis, evaluation function based on the trade-off between slip suppression performance and chattering reduction performance is proposed. The analyses are conducted in several numerical simulations of slip suppression problem of EVs. Then, we can see that there is no difference of employed candidate functions in chattering reduction performance. On the other hand, in slip suppression performance, the saturation function is excellent overall. So, we conclude the saturation function is most suitable for slip suppression sliding mode control.

Keywords—Sliding mode control, chattering function, electric vehicle, slip suppression, performance analysis.

I. INTRODUCTION

IN this century, automobiles have become popular all over the world and the number of automobiles has been increasing rapidly, especially in the developing countries. With such wide spread of internal-combustion engine vehicles (ICEVs) all over the world, the environment and energy problems: air pollution, global warming, and so on, are going severely [1]. In this situation, therefore, the development of next-generation vehicles, for example, electric vehicles (EVs) and so on, is very important. EVs run are zero emission and eco-friendly. So EVs have attracted great interests as one of the powerful solution against the problems mentioned above [2].

EVs are driven by electric motors and electric motors have several advantages over ICEs:

- 1) The motor torque response between input and output is hundreds of times faster than that of gasoline/diesel engines.
- 2) Since we can detect the wheel torque in EV accurately and easily, it is possible to accurate and quick drive control for EV. On the other hands, the wheel torque of ICEV has high-nonlinearity due to the temperature

S. Horikoshi was with Department of Computer Science, Graduate School of Systems and Information Engineering, University of Tsukuba, Tsukuba 305-8573 Japan.

T. Kawabe is with the Division of Information Engineering, Faculty of Engineering, Information and Systems University of Tsukuba, Tsukuba 305-8573 Japan (phone: +81-29-853-5507; e-mail: kawabe@cs.tsukuba.a.jp).

and revolutions. Therefore, it's difficult to measure the accurate value of the torque in ICEVs. However, the value of motor torque is surveyed easily and accurately from

- 3) The vehicle bodies can be made smaller by using multiple motors set into each wheels, if each wheels can be controlled to drive independently.

There have been several research results about various vehicle control methods, e.g., Anti-lock-Braking Systems (ABS), Traction-Control-Systems (TCS), Electric-Stability-Control (ESC) [3], Vehicle-Stability-Assist (VSA) [4], All-Wheel-Control (AWC) [5], and so on. The objective of these methods in common is to maintain a suitable tire grip margin and to improve the driving performance. But, the response time between the driving torque input and the tire force transmitted to the wheels is slow in the case of vehicles with gasoline/diesel engines. Therefore such vehicles limit the control performance.

On the other hands, EVs have a fast torque response and the motor characteristics can be used to accurately determine the torque, which makes it relatively easy and inexpensive to realize high-performance traction control. Then, several methods have been proposed for the traction control [6]-[8] by using slip ratio of EVs, such as the method based on Model Following Control (MFC) in [6]. We have been proposed conventional Sliding Mode Control (SMC) based method [9].

However, for slip suppression with the conventional SMC [10], the control performance will get degradation due to the chattering which always occurs when switching the control inputs due to the structure of SMC. To overcome such disadvantages, we have also proposed the extended SMC method, so-called SMC-I, introducing the integral action with gain to design the sliding surface in [11]. Although we employ the general saturation function for chattering reduction in this method, the performance could not be enough. In order to get better control performance, we need to solve such problem.

This paper, therefore, several candidate functions for chattering reduction are selected and control performance of SMC with candidate functions is analyzed. In the analysis, evaluation function based on the trade-off between slip suppression performance and chattering reduction performance is proposed. The analyses are conducted in several numerical simulations of slip suppression problem of EVs.

II. SLIDING MODE CONTROL

A. Basic Concept of SMC

SMC (sliding Mode Control) is one of the VSC (Variable Structure Control) methods in 1970's [12], [13]. From 1980's,

with the improvement of computer performance, SMC is applied in many control fields such as high-precision motor control [14], automotive control [15] and robot attitude control [16]. Now SMC is considered as an effective nonlinear-robust control method and have been attracted more and more attention. SMC utilizes discontinuous feedback control laws to force the system trajectory to reach, and subsequently to remain on a specified surface within the state space (it's so called sliding or switching surface). For example, consider the single input nonlinear system [17].

$$\dot{x}^{(n)} = f(\mathbf{x}) + b(\mathbf{x})u \quad (1)$$

where u is the control input and $\mathbf{x} = [x \ \dot{x} \ \dots \ x^{(n-1)}]^T$ is the state vector. In general, the function $f(\mathbf{x})$ and the control gain $b(\mathbf{x})$ are nonlinear. In (1), $f(\mathbf{x})$ and $b(\mathbf{x})$ are not exactly known, but the extents of the imprecision on $f(\mathbf{x})$ and $b(\mathbf{x})$ are upper bounded by known continuous functions of \mathbf{x} . The control problem is to seek a control law that makes the state \mathbf{x} to track the desired state $\mathbf{x}^* = [x^* \ \dot{x}^* \ \dots \ x^{*(n-1)}]^T$ in the presence of model imprecision on $f(\mathbf{x})$ and $b(\mathbf{x})$.

Let us define a time-varying surface $S(t)$ in the state space $\mathbf{R}^{(n)}$ by the equation $s(\mathbf{x};t)$ defined as follow,

$$S(t) = \{x | s(\mathbf{x};t) = 0\} \quad (2)$$

where $s(\mathbf{x};t)$ is defined by

$$s(\mathbf{x};t) = \left(\frac{d}{dt} + \alpha\right)^{n-1} \mathbf{x}_e, \quad \alpha > 0 \quad (3)$$

where $\mathbf{x}_e = \mathbf{x} - \mathbf{x}^* = [x_e \ \dot{x}_e \ \dots \ x_e^{(n-1)}]^T$ indicates the error between the output state and the desired one. The tracking problem of $\mathbf{x} \equiv \mathbf{x}^*$ is equivalent to remain on the surface $S(t)$ for all $t > 0$. From (3), $s \equiv 0$ presents a linear differential equation whose unique solution is $\mathbf{x}_e \equiv 0$. Thus, the problem of tracking the n -dimensional vector \mathbf{x}^* can be replaced by a 1st order stabilization problem in s . When $s(\mathbf{x};t)$ equals 0, that is to say, the system trajectories reach the surface which represents the tracking error is 0. Here, $S(t)$ is known as sliding surface. On this surface, the error will converge to 0 exponentially.

B. Implementation of SMC

In general, to design a control system based on SMC should go through the following two steps:

- Design a sliding surface that is invariant of the controlled dynamics.
- Define the control input that drives the system trajectory to the sliding surface in sliding mode in finite time.

Considering the system equation (1) defined in the previous section, assume that for all x , $b(\mathbf{x}) \neq 0$. We derive a control such that $\dot{s} = 0$ when the sliding mode exists, (3) can be rewrite as

$$s = x_e^{(n-1)} + \dots + \alpha^{n-1} x_e. \quad (4)$$

Differentiate equation (4), we can obtain that

$$\begin{aligned} \dot{s} &= \dot{x}_e^{(n)} + \dots + \alpha^{n-1} \dot{x}_e \\ &= \dot{x}^{(n)} - \dot{x}^{*(n)} + \dots + \alpha^{n-1} \dot{x}_e \\ &= f(\mathbf{x}) + b(\mathbf{x})u - \dot{x}^{*(n)} + \dots + \alpha^{n-1} \dot{x}_e \end{aligned} \quad (5)$$

while the dynamics is in sliding mode,

$$\dot{s} = 0. \quad (6)$$

By solving the equation for the control input, $u = u_{eq}$,

$$u_{eq} = \frac{1}{b(\mathbf{x})} (-f(\mathbf{x}) + \dot{x}^{*(n)} - \dots - \alpha^{n-1} \dot{x}_e). \quad (7)$$

Here, u_{eq} is called the equivalent control input, which can be interpreted as the control law that would maintain $\dot{s} = 0$ if the dynamics were in the sliding mode. However, if the system trajectory is not on the sliding surface (the reaching mode), an another item has to be added to the control input to drive the system to the sliding surface. In the reaching mode, the switching control u_{sw} makes the trajectory from the initial trajectory to the sliding surface and it can be defined as

$$u_{sw} = -\frac{K}{b(\mathbf{x})} \text{sgn}(s) \quad (8)$$

where

$$\text{sgn}(s) = \begin{cases} -1, & s < 0 \\ 0, & s = 0 \\ 1, & s > 0 \end{cases} \quad (9)$$

and K is called sliding gain.

In (8), the switching control using the discontinuous function requires infinitely fast switching, but in real systems, the sampling and delays in digital implementation causes s to pass to the other side of the surface $S(t)$, which produces chattering. Chattering is high-frequency finite oscillations which is caused by switching of the variable s around the sliding surface $S(t)$. That's the point. For reducing the chattering, it is conceivable to adopt a function $\text{sat}\left(\frac{s}{\Phi}\right)$ is defined as

$$\text{sat}\left(\frac{s}{\Phi}\right) = \begin{cases} -1, & s < -\Phi \\ \frac{s}{\Phi}, & -\Phi \leq s \leq \Phi \\ 1, & s > \Phi \end{cases} \quad (10)$$

where $\Phi > 0$ is a design parameter representing the width of the boundary layer around the sliding surface $s = 0$. With this replacement, the sliding surface function s with an arbitrary initial value will reach and stay within the boundary layer $|s| \leq \Phi$.

From (8), the switching control is rewritten as

$$u_{sw} = -\frac{K}{b(\mathbf{x})} \text{sat}\left(\frac{s}{\Phi}\right). \quad (11)$$

Finally, the SMC control law can be defined as

$$\begin{aligned} u &= u_{eq} + u_{sw} \\ &= \frac{-1}{b(\mathbf{x})} \left(f(\mathbf{x}) - \dot{x}^{*(n)} + \dots + \alpha^{n-1} \dot{x}_e + K \text{sat}\left(\frac{s}{\Phi}\right) \right) \end{aligned} \quad (12)$$

In summary, when the trajectory is on the sliding surface ($s = 0$), it is desired to have $u_{sw} = 0$, the switching control has no effect on the sliding surface. Moreover, when the trajectory

is off the sliding surface or the uncertainty in the system occurs, the switching control acts to return the trajectory back to the sliding surface. Therefore, the total control u causes the system to keep the trajectory on the sliding surface.

III. ELECTRIC VEHICLE DYNAMICS

A. One Wheel Car Model

As a first step toward practical application, this paper restricts the vehicle motion to the longitudinal direction and uses direct motors for each wheel to simplify the one-wheel model to which the drive force is applied. In addition, braking was not considered this time with the subject of the study being limited to only when driving.

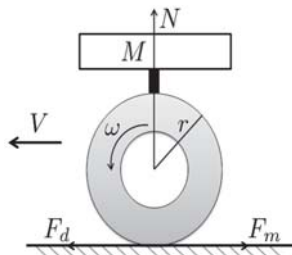


Fig. 1 One-wheel car model

From Fig. 1, the vehicle dynamical equations are expressed as (13)-(15).

$$M \frac{dV}{dt} = -F_d(\lambda) + F_a \quad (13)$$

$$J \frac{d\omega}{dt} = rF_d(\lambda) - T_b \quad (14)$$

$$F_d = \mu(c, \lambda)N \quad (15)$$

where M is the vehicle weight, V is the vehicle body velocity, F_d is the driving force, J is the wheel inertial moment, F_a is the resisting force from air resistance and other factors on the vehicle body, T_b is the braking torque, ω is the wheel angular velocity, r is the wheel radius, c is road surface condition coefficient, and λ is the slip ratio. The slip ratio of the wheel is defined as the difference between the wheel and body velocities, divided by the maximum of these velocity values (wheel velocity for acceleration, vehicle body velocity for braking), and given by

$$\lambda = \begin{cases} \frac{V_\omega - V}{V_\omega} & \text{(accelerating)} \\ \frac{V - V_\omega}{V} & \text{(braking)} \end{cases} \quad (16)$$

The value of $\lambda = 0$ characterizes the free motion of the wheel where no wheel slip happens (no friction force is exerted). If the slip attains the value $\lambda = 1$, then the wheel is completely skidding. The friction forces that are generated between the road surface and the tires are the force generated in the longitudinal direction of the tires and the lateral force acting perpendicularly to the vehicle direction of travel, and both of these are expressed as a function of λ . The friction force generated in the tire longitudinal direction is expressed

as μ , and the relationship between μ and λ is shown by (17) below, which is a formula called the **Magic-Formula** and gives values compatible with experimental data given in [18]. It is simplified and has been using in earlier study in [19].

$$\mu(c, \lambda) = -c \times 1.1 \times (e^{-35\lambda} - e^{-0.35\lambda}) \quad (17)$$

where c is the coefficient used to determine the road condition and was found by experimental data to be approximately $c = 0.8$ for general dry asphalt roads, approximately $c = 0.5$ for general wet asphalt roads, and approximately $c = 0.12$ for icy road. In the simulations, this formula is used for estimating the maximum value of friction coefficient.

The $\mu - \lambda$ curve for acceleration case is shown in Fig. 2 on three different road conditions (dry asphalt, wet asphalt and icy road). It shows how the friction coefficient μ increases with slip ratio λ up to a value λ^* ($0.1 < \lambda^* < 0.2$) where it attains the maximum value of the friction coefficient. As defined in (15), the driving force also achieves the maximum value in corresponding to the friction coefficient. However, the friction coefficient decreases to the minimum value when the wheel is completely skidding. Therefore, to achieve the maximum value of driving force for slip suppression, λ should be maintained at the desired value λ^* . The value of λ^* is derived as follows.

Choose the function $\mu_c(\lambda)$ defined as

$$\mu_c(\lambda) = -1.1 \times (e^{-35\lambda} - e^{-0.35\lambda}). \quad (18)$$

By using equation (18), Equation (17) can be rewritten as

$$\mu(c, \lambda) = c \cdot \mu_c(\lambda). \quad (19)$$

Evaluating the values of λ which maximize $\mu(c, \lambda)$ for different $c (c > 0)$, means to seek the value of λ where the maximum value of the function $\mu_c(\lambda)$ can be obtained. Then let

$$\frac{d}{d\lambda} \mu_c(\lambda) = 0 \quad (20)$$

and solving equation (20) gives

$$\lambda = \frac{\log 100}{35 - 0.35} \approx 0.13. \quad (21)$$

Therefore, for the different road conditions, when $\lambda \approx 0.13$ is satisfied, the maximum driving force can be gained. Namely, from (17) combined with Fig. 2 we find that regardless of the road condition (value of c), the $\mu - \lambda$ surface attains the largest value of μ when λ is the optimal value 0.13. So in this dissertation, desired value of slip ratio is set by $\lambda^* = 0.13$.

IV. SMC WITH INTEGRAL ACTION FOR SLIP SUPPRESSION

In this section, the previous proposed control strategy based on SMC with integral action (SMC-I) [11] is explained. Without loss of generality, one wheel car model in Fig. 1 is used for the design of the control law. The nonlinear system dynamics can be presented by a differential equation as

$$\dot{\lambda} = f + bT_m \quad (22)$$

where $\lambda \in R$ is the state of the system representing the slip ratio of the driving wheel which is defined as (16) for the

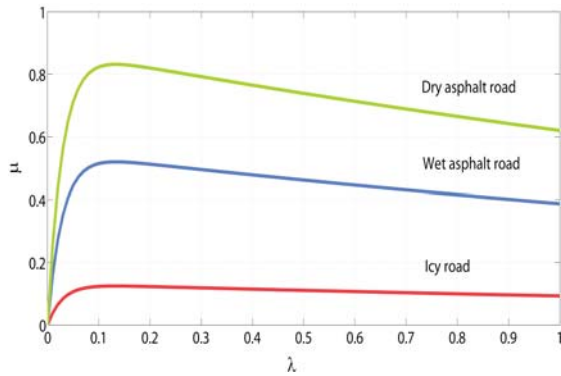


Fig. 2 $\mu - \lambda$ curve

case of acceleration, $T_m \in R$ is the control input representing the torque of the motor. f describes the nonlinearity of system and b is the input gain, and they are all time-varying. Differentiating (16) for the case of acceleration with respect to time gives

$$\dot{\lambda} = \frac{-\dot{V} + (1-\lambda)\dot{V}_w}{V_w} \quad (23)$$

Then, the system dynamics can be rewritten as

$$\dot{\lambda} = -\frac{g}{V_w} \left[1 + (1-\lambda) \frac{r^2 M}{J_w} \right] \mu(c, \lambda) + \frac{(1-\lambda)r}{J_w V_w} T_m. \quad (24)$$

By reference to the system dynamics, the following equations can be attained,

$$f = -\frac{g}{V_w} \left[1 + (1-\lambda) \frac{r^2 M}{J_w} \right] \mu(c, \lambda), \quad (25)$$

$$b = \frac{(1-\lambda)r}{J_w V_w}. \quad (26)$$

The sliding mode controller is described to maintain the value of slip ratio λ at the desired value λ^* .

Referring to [11], in order to reduce the undesired chattering effect for which it is possible to excite high frequency modes, and guarantee zero steady-state error, an integral action with gain has been introduced to the design of sliding surface. By adding an integral item to the difference between the actual and desired values of the slip ratio, the sliding surface function s is given by

$$s = \lambda_e + K_{in} \int_0^t \lambda_e(\tau) d\tau, \quad (27)$$

where λ_e is defined as $\lambda_e = \lambda - \lambda^*$ and K_{in} is the integral gain, $K_{in} > 0$.

The sliding mode occurs when the state reaches the sliding surface defined by $s = 0$. The dynamics of sliding mode is governed by

$$\dot{s} = 0. \quad (28)$$

By using (22)-(28), the sliding mode control law is derived by adding a switching control input T_{msw} to the nominal equivalent control input T_{meq_n} as in [11]

$$T_m = T_{meq_n} + T_{msw}, \quad (29)$$

$$T_{meq_n} = \frac{1}{b} [-f_n - K_{in} \lambda_e], \quad (30)$$

$$T_{msw} = \frac{1}{b} \left[-K \text{sat} \left(\frac{s}{\Phi} \right) \right], \quad (31)$$

where “ n ” is used to indicate the estimated model parameters. f_n is the estimation of f calculated by using the nominal values of vehicle mass M_n and road surface condition coefficient c_n . $\Phi > 0$ is a design parameter which defines a small boundary layer around the sliding surface. The sliding gain $K > 0$ is selected as

$$K = F + \eta \quad (32)$$

by defining Lyapunov candidate function in [11], where $F = |f - f_n|$ and η is a design parameter.

By using (29), (30), (31) and (32), the control law of SMC-I can be represented as

$$T_m = \frac{1}{b} \left[-f_n - K_{in} \lambda_e - (F + \eta) \text{sat} \left(\frac{s}{\Phi} \right) \right]. \quad (33)$$

In this method, standard saturation function, $\text{sat} \left(\frac{s}{\Phi} \right)$ in (10), was employed.

V. ANALYSIS OF CONTROL PERFORMANCE

A. Candidates for Chattering Function

The switching control input using the sign function in (9) is used theoretically. But, in real systems, the sampling and delays in digital implementation causes s to pass to the other side of the surface $S(t)$, which produces chattering. A solution to reduce this chattering introduces a region around $S(t)$ called boundary layer so that s changes its value continuously [17]. The boundary layer is realized to use “S-shape type” function replacing $\text{sgn}(s)$. Since the trajectory in the boundary layer varies depend on the used function, the chattering reduction performance is different. Hereinafter the function of the S-shape type used for boundary layer introduction is called the chattering reduction function. In this paper, L_0 , L_1 , L_2 and L_3 shown in (37) are considered as candidates of the chattering function,

$$L_0 = \begin{cases} -1 & (s < -\Phi) \\ \frac{s}{\Phi} & (-\Phi \leq s \leq \Phi) \\ 1 & (s > \Phi) \end{cases} \quad (34)$$

$$L_1 = \frac{s}{|s| + \delta} \quad (35)$$

$$L_2 = \tanh \left(\frac{\sigma s}{2} \right) \quad (36)$$

$$L_3 = 2 \times \left(\frac{1}{2} \right)^{b^s} - 1 \quad (37)$$

where $\Phi \delta \sigma b (0 < b < 1)$ are design parameters related to the width of boundary layer.

L_0 is Saturation function, and it's same as (10). In this function, the width of the boundary layer becomes narrow so as to smaller the value of Φ . L_1 is Smooth function. In this function, the width of the boundary layer becomes narrow so as to smaller the value of δ . L_2 is Bipolar function. In this function, the width of the boundary layer becomes narrow so

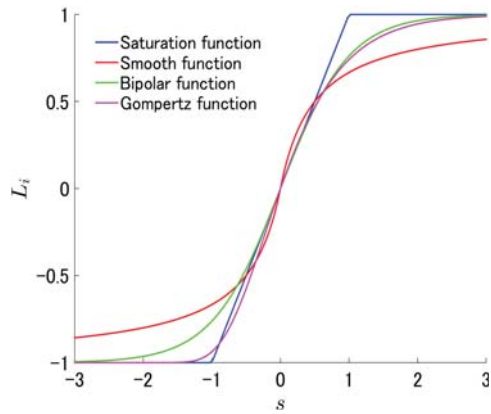


Fig. 3 Candidate functions

as to bigger the value of σ . L_3 is Gompertz function and its asymmetry. In this function, the width of the boundary layer becomes narrow so as to smaller the value of b . The chattering reduction performance of these four functions are analyzed. These four functions are shown in Fig. 3. Values of parameters in each function are tuned as $\Phi = 1.0$, $\delta = 0.5$, $\sigma = 2.0$, $b = 0.2$ for visibility.

B. Evaluation Index for Control Performance

The index to compare the performance of 4 candidate functions is considered. It can be said that there is generally a relation of a trade-off in the slip suppression performance and the chattering reduction performance in slip suppression problem by using SMC. Therefore, it is desirable to reduce chattering of the driving torque without deteriorating slip suppression performance. From this fact, the following evaluation index is introduced.

$$J = k_c C + k_e E \quad (38)$$

where $C = \max \left| \frac{dT_m}{dt} \right|$, $E = \int_0^{t_f} |\tilde{\lambda}| dt$ and where k_c and k_e are design parameters. C is a maximum value of gradient of driving torque. The amplitude of the vibration of the driving torque could be gently suppressed small by holding down of C small. In other words, smaller value of C means higher chattering reduction performance. On the other hands, E indicates the accumulated error with the value and the target value of slip rate from simulation starting to the end. Namely, smaller value of E means higher slip suppression performance.

Then, the chattering reduction performance and slip suppression performance of L_0 , L_1 , L_2 and L_3 are analyzed by calculating the minimum value of this J with changing the value of parameters in these functions, Φ , δ , σ , b , respectively.

C. Performance Analysis by Simulations

In simulations, we consider three different road conditions, a dry asphalt, a wet asphalt and an icy road. As the input to the simulation of system, the driving torque is produced by the constant pressure on the accelerator pedal, which is decided on the vehicle speed desired by the driver. Here, the vehicle speed is desired to achieve $180[km/h]$ in $15[s]$ by a

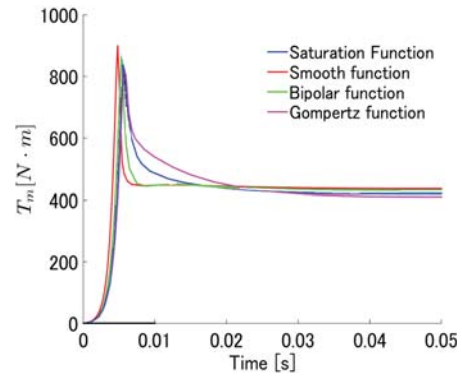


Fig. 4 Enlarged view of time response of driving torque on wet asphalt ($0 < t < 0.05$)

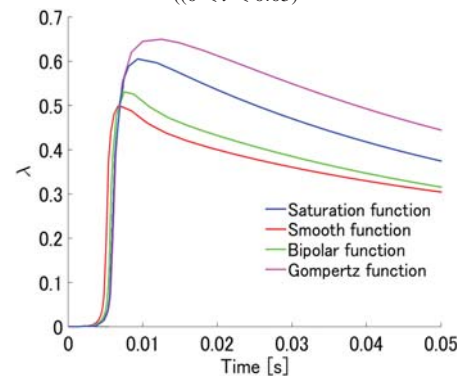


Fig. 5 Enlarged view of time response of slip ratio on wet asphalt ($0 < t < 0.05$)

fixed acceleration after starting the car. The range of variation in mass of vehicle M and road condition coefficient c are imposed as $M_{max} = 1400[kg]$, $M_{min} = 1000[kg]$, $c_{max} = 0.9$ and $c_{min} = 0.1$ respectively. So the nominal values of mass and road condition coefficient can be obtained as $\hat{M} = 1200[Kg]$ and $\hat{c} = 0.5$.

The values of design parameters are set as Table I. These values are obtained by trial and error search in preliminary simulations and they lowered the value of J .

	Dry	Wet	Icy
Φ in Saturation function(L_0)	0.60	0.97	1.34
δ in Smooth function(L_1)	0.41	0.30	0.36
σ in Bipolar function(L_2)	3.73	3.10	1.68
b in Gompertz function(L_3)	0.07	0.24	0.27

[a] *Results on dry asphalt*($c = 0.8$) From time responses of driving torque and slip ratio on dry asphalt simulations, we cannot the differences in both responses of driving torque and slip ratio with all functions.

[b] *Results on wet asphalt*($c = 0.5$)

Time responses of driving torque and slip ratio on wet asphalt are shown in Figs. 4 and 5, respectively. These figures show only the first section ($0 < t < 0.05$) with the conspicuous difference was expanded is indicated. From these figures, we can see that there is no difference in the chattering reduction

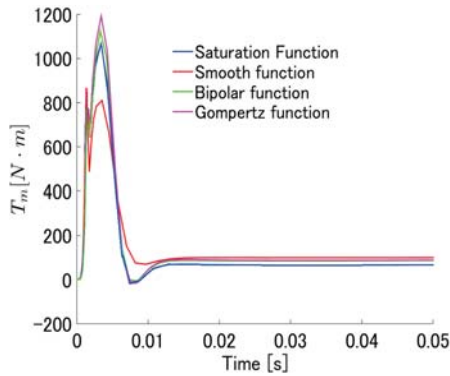


Fig. 6 Enlarged view of time response of driving torque on icy road (($0 < t < 0.05$))

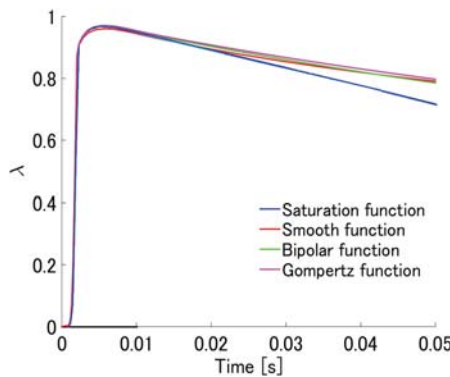


Fig. 7 Enlarged view of time response of slip ratio on icy road (($0 < t < 0.05$))

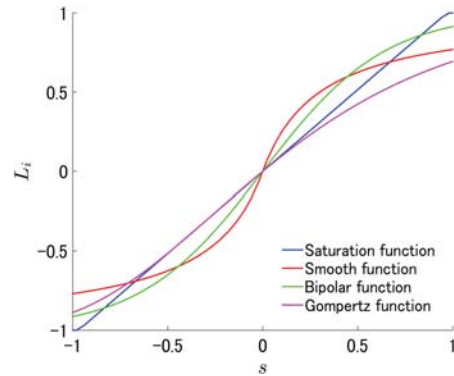


Fig. 8 Candidate functions on wet asphalt

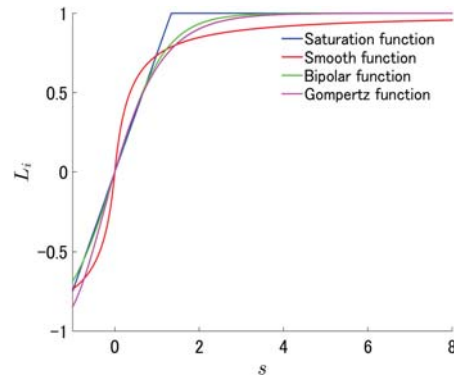


Fig. 9 Candidate functions on icy road

performance. But, we see the time responses of driving torque and slip ratio with gompertz function are slightly inferior to other functions, especially in first transient section. It shows slow convergence compared with the other functions. Smooth function is slightly good among all.

[c] Results on icy road ($c = 0.12$)

Time responses of driving torque and slip ratio on icy road in the first section ($0 < t < 0.05$) are shown in Figs. 6 and 7 respectively. From these figures, also we can not see the difference in the chattering reduction. The time responses of driving torque with saturation function seems to be slightly bad, since it shows large oscillatory reaction compared with the other functions, especially in first transient section. On the other hands, saturation function shows superior response in both response of driving torque and slip ratio to other functions.

[d] Discussion

Although there is difference according to the road surface conditions, it can maybe have said that saturation function is excellent overall from simulation results. The reason is considered from the shape of each function using wet asphalt and the icy road cases.

In Fig. 8, the absolute values of gompertz function in the section of $s > 0.5$ are smaller than the other functions. Namely, the values of gompertz function away from the top value, compared with other functions. Therefore, the effect of bringing the state close to the switching surface is weak. This

makes bigger the value of E in J and worse the performance of slip suppression. On the other hands, smooth function has bigger value than the one of other functions at the around of $s = -1$ and the rate of change is big through the whole compared with others. It seems that this well-controlled change of saturation function makes good effect to performances of driving torque and slip ratio.

From Fig. 9, we can see that the saturation function strictly reach the value of 1 rather faster than other functions. Other functions do not reach the value of 1 strictly. This means that the effect of bringing the state close to the switching surface of the other functions is rather weak than the one of saturation function. Therefore, the saturation function shows superior performance of slip suppression among all.

VI. CONCLUSION

In this paper, we present the performance analysis results of SMC with changing the chattering functions applied to slip suppression problem of EVs. The function of the following 4 was chosen as a candidate; saturation function (L_0), smooth function (L_1), bipolar function (L_2) and gompertz function (L_3). They are all "S-shape type" function. The performance of SMC with each function is analyzed in slip suppression problem of EVs. Firstly, the evaluation index (J) taking into the trade-off relation in the slip suppression performance and the chattering reduction performance has been proposed for this purpose. Then, we analyze the control performance of SMC with 4 candidate functions by this index from simulations with three different road conditions, a dry asphalt

a wet asphalt and an icy road. As a result, we can see that there is no difference of 4 functions in chattering reduction performance, and that saturation function is excellent overall in slip suppression performance. Therefore, we conclude the saturation function is most suitable for slip suppression sliding mode control. In future works, it is need to extend the SMC with saturation function improving the control performance for practical use, for example, introducing the approach angle for saturation function.

ACKNOWLEDGMENTS

This research was partially supported by Grant-in-Aid for Scientific Research (C) (Grant number: 16K06409; Tohru Kawabe; 2016-2018) from the Ministry of Education, Culture, Sports, Science and Technology of Japan.

REFERENCES

- [1] A. G. Mamalis, K. N. Spentzas and A. A. Mamali, The Impact of Automotive Industry and Its Supply Chain to Climate Change: Somme Techno-economic Aspects, *European Transport Research Review*, Vol.5, No.1, 2013, pp.1–10.
- [2] H. Tseng and J. S. Wu and X. Liu, Affordability of Electric Vehicle for a Sustainable Transport System: An Economic and Environmental Analysis, *Energy Policy*, Vol.61, 2013, pp.441–447.
- [3] A. T. Zanten, R. Erhardt and G. Pfaff, VDC; The Vehicle Dynamics Control System of Bosch, *Proc. Society of Automotive Engineers International Congress and Exposition*, 1995, Paper No. 950759.
- [4] K. Kin, O. Yano and H. Urabe, Enhancements in Vehicle Stability and Steeringability with VSA, *Proc. JSME TRANSLOG 2001*, 2001, pp.407–410 (in Japanese).
- [5] K. Sawase, Y. Ushiroda and T. Miura, Left-Right Torque Vectoring Technology as the Core of Super All Wheel Control (S-AWC), *Mitsubishi Motors Technical Review*, No.18, 2006, pp.18–24 (in Japanese).
- [6] S. Kodama, L. Li and H. Hori, Skid Prevention for EVs based on the Emulation of Torque Characteristics of Separately-wound DC Motor, *Proc. The 8th IEEE International Workshop on Advanced Motion Control*, VT-04-12, 2004, pp.75–80.
- [7] M. Mubin, S. Ouchi, M. Anabuki and H. Hirata, Drive Control of an Electric Vehicle by a Non-linear Controller, *IEEJ Transactions on Industry Applications*, Vol.126, No.3, 2006, pp.300–308 (in Japanese).
- [8] K. Fujii and H. Fujimoto, Slip ratio control based on wheel control without detection of vehicle speed for electric vehicle, *IEEJ Technical Meeting Record*, VT-07-05, 2007, pp.27–32 (in Japanese).
- [9] S. Li, K. Nakamura, T. Kawabe and K. Morikawa, A Sliding Mode Control for Slip Ratio of Electric Vehicle, *Proc. of SICE Annual Conference 2012*, pp.1974–1979.
- [10] I. Eker and A. Akinal, Sliding Mode Control with Integral Augmented Sliding Surface: Design and Experimental Application to an Electromechanical system, *Electrical Engineering*, Vol.90, 2008, pp.189–197.
- [11] S. Li and T. Kawabe, Slip Suppression of Electric Vehicles Using Sliding Mode Control Method, *International Journal of Intelligent Control and Automation*, Vol.4, No.3, 2013, pp.327–334.
- [12] V. Utkin, Variable Structure Systems with Sliding Modes, *IEEE Transactions on Automatic Control*, Vol. 22, No. 2, 1977, pp. 212-222.
- [13] V. Utkin, *Sliding Modes and Their Applications in Variable Structure Systems*, Mir Publishers, USSR, 1978.
- [14] U. M. Ch, Y. S. K. Babu and K. Amaresh, Sliding Mode Speed Control of a DC Motor, *Proc. of 2011 International Conference on Communication Systems and Network Technologies*, 2011, pp. 387-391.
- [15] K. Nakano, U. Sawut, K. Higuchi and Y. Okajima, Modelling and Observer-based Sliding-mode Control of Electronic Throttle Systems, *Transaction on Electrical Engineering, Electronics and Communications*, Vol. 4, No. 1, 2006, pp. 22-28.
- [16] Y. Li, J. O. Lee and J. Lee, Attitude Control of the Unicycle Robot Using Fuzzy-sliding Mode Control, *Proc. of the 5th International Conference on Intelligent Robotics and Applications*, Vol. 3, 2012, pp. 62-72.
- [17] J. E. Slotine, W. Li, *Applied Nonlinear Control*, Prentice Hall, 1991, USA.
- [18] H. B. Pecejka and E. Bakker, The Magic Formula Tyre Model, *Proc. of the 1st International Colloquium on Tyre Models for Vehicle Dynamics Analysis*, 1991, pp. 1-18.
- [19] Y. Hori, Simulation of MFC-Based Adhesion Control of 4WD Electric Vehicle, *IEEJ Record of Industrial Measurement and Control*, Vol. IIC-00, No. 1-23, 2000, pp. 67-72 (in Japanese).